Acadlore Transactions on Applied Mathematics and Statistics
https://www.acadlore.com/journals/ATAMS

Mathematical Analysis of the Fractal-Fractional Nanofluid Model for Heat Transfer Enhancement in Polystyrene/Kerosene Oil Systems

Saqib Murtaza[1*], Razi Khan[2], Zubair Ahmad[3]

[1] Department of Mathematics, King Mongkut's University of Technology, 10140 Bangkok, Thailand
[2] Department of Mathematics and CEMAT, Instituto Superior Tecnico, 1049-001 Lisbon, Portugal
[3] Dipartimento di Matematica e Fisica, Universit'a degli Studi della Campania "Luigi Vanvitelli", 81100 Caserta, Italy

[*] Correspondence: Saqib Murtaza (saqib.murtaza@mail.kmutt.ac.th)

Received: 09-25-2024 **Revised:** 11-08-2024 **Accepted:** 12-16-2024

Citation: S. Murtaza, R. Khan, and Z. Ahmad,, "Mathematical analysis of the fractal-fractional nanofluid model for heat transfer enhancement in polystyrene/kerosene oil systems," *Acadlore Trans. Appl Math. Stat.*, vol. 2, no. 4, pp. 180–192, 2024. https://doi.org/10.56578/atams020401.

Abstract: Nanofluids, which are suspensions of nanoparticles in base fluids, have demonstrated considerable potential in enhancing thermal conductivity, energy storage, and lubrication properties, as well as improving the cooling efficiency of electronic devices. Despite their promising applications, the industrial utilization of nanofluids remains in the early stages, with further research needed to fully explore their capabilities. This study investigates a generalized nanofluid model, incorporating fractal-fractional derivative (FFD), to better understand the thermophysical behaviors in vertical channel flow. The nanofluid consists of polystyrene nanoparticles uniformly dispersed in kerosene oil. An exact solution to the model is obtained by employing the Laplace transform technique (LTT) in combination with the numerical Zakian's algorithm. The FFD operator with an exponential kernel is applied to extend the classical nanofluid model. Discretization of the generalized model is achieved using the Crank-Nicolson method, and numerical simulations are performed to solve the resulting equations. The study reveals that, at a nanoparticle volume fraction of 4% (0.04), the heat transfer rate of the nanofluid is significantly higher than that of the base fluid. Furthermore, the enhanced heat transfer leads to improvements in various thermophysical properties, such as viscosity, thermal expansion, and heat capacity, which are crucial for industrial applications. The numerical results are presented graphically to highlight the dependence of the flow and thermal dispersion characteristics on key physical factors. These findings suggest that the use of fractal-fractional models can provide a more accurate representation of nanofluid behavior, particularly for high-precision applications in heat transfer and energy systems.

Keywords: Fractal-fractional derivative (FFD); Polystyrene nanocomposite; Integral transform technique; Zakian's algorithm

1 Introduction

Researchers are actively seeking a way to enhance the thermal properties of the regular fluids due to their significant uses in many industries. With the passage of time, many ideas are presented in the research community to enhance the heat transfer of the regular fluid, but suspension of solid particles in the base fluid was the most used among them. In 1864, the idea of microsize particles was presented in the research community. At the start, this idea was used by many engineers and obtained the required results. But after some time, the disadvantage came to know that microparticles cause clogging and sedimentation in the fluid, and then it cannot be tailored to specific requirements. In 1995, two scientists from Argonne National Laboratory, USA, came up with the idea of suspension of nanoparticles in the base fluid, and this idea took the research community by storm. Nanofluid emerged as a frontier in the fluid industry, offering advanced thermal properties as compared to regular fluids. These advanced thermal properties improve the heat transfer capabilities of base fluids. The significance of nanofluids can be found in various fields; it spans various applications, from industrial cooling systems to diagnosis of diseases and drug delivery, etc., that show the potential to revolutionize multiple industries [1–3]. In the literature, various types of nanoparticles exist, each with distinctive qualities that make them different in their respective sectors. Polystyrene nanoparticles are notable examples among them. Due to their unique ease of production and chemical stability,

polystyrene nanoparticles are extensively used in the development of nanofluids [4, 5]. The integration of these nanoparticles into base fluids is pivotal in the advancement of overall performance and thermal management of nanofluids. This nanoparticle is also gaining attention in fuel technology, especially augmenting the characteristics of kerosene oil. These nanoparticles are valued for their ability to improve the thermal conductivity and combustion efficiency of kerosene, a commonly used fuel in both aviation and heating. When polystyrene nanoparticles are dispersed in kerosene, they modify the fuel's burning characteristics, leading to more complete combustion [6–10]. Li et al. [11] established an efficient method for identifying polystyrene nanoparticles in ambient waterways, which allows contamination levels to be monitored. Mebarek-Oudina et al. [12] investigated the hydromagnetic flow of magnet nano-water by using the adapted Buongiorno model. They analyzed the model by using the numerical algorithm of RK4. Li et al. [13] discussed various aspects of induced magnetic field for the utilization of heat and mass transfer enhancement of hybrid nanofluid. Ajmal et al. [14] investigated numerically the electroosmotic peristaltic flow of Casson nanofluid for optimizing the heat transfer of blood flow with Cu (Copper) characteristics. For numerical simulation, the authors used the bvp4c technique. They have been found that the temperature profile increased with an increase in the volumetric percentage of nanoparticles. Nabawey et al. [15] theoretically examined the heat and mass transfer in micropolar, Maxwell, and Williamson nanofluid flow. The investigation has been numerically with the help of the fourth-order RK method. From their analysis, they concluded that the Nusselt number increases with the increase in the magnitude of the Prandtl number. The exact solution of the mathematical model of hybrid nanofluid flow that is flowing across a heated stretching cylinder was found by Usman et al. [16]. The authors considered two different nanoparticles, Cooper and aluminum oxide, and base fluid water for their hybrid nanofluid preparation. Other interesting studies on the significance of nanofluids can be found in the studies [17–21].

Fractal-fractional calculus is an advanced mathematical tool that combines the concepts of fractal and fractional calculus [22]. Its importance arises from its ability to model complicated systems more precisely than classical derivatives. The FFD has a number of important consequences for nanofluids, which are nanoparticle suspensions in base fluids. First, it allows for better modeling of complicated dynamics. Nanofluids frequently exhibit anomalous properties, such as odd viscosity or thermal behavior, which traditional models cannot account for. The FFD, on the other hand, handles these behaviors better because of its capacity to manage nonlinearity and scale-dependent features [23]. Furthermore, this derivative is very effective when studying multi-scale phenomena, which is critical because nanofluids act at multiple scales. For example, heat transport at the nanoparticle level is distinct from macroscopic processes. This fractal-fractional technique provides a seamless connection across these levels. Moreover, due to the interaction between the nanoparticle and the base fluid, nanofluids generally show memory effects and irregular diffusion. FFDs have a memory term that is simply able to catch these any things, but this will be exceptionally difficult using traditional (integer) order derivatives. Additionally, the FFD increases conduction and convection heat modeling. The application of nanofluids is highly dependent on the knowledge and predictability of their behavior as heat transfer enhancers in an array of devices. A validated model utilizing this method could result in the development of more efficient cooling/heating systems. Finally, models based on this derivative can optimize industrial processes involving nanofluids, such as those in chemical reactors, heat exchangers, and biomedical devices [24]. Given the significance of FFDs in nanofluids, Asifa et al. [25] showed that a fractal-fractional model with varied nanoparticle shapes enhances heat conduction by up to 9.58% in an engine oil nanofluid. Murtaza et al. [26] demonstrated that this approach improves heat and mass transport in cadmium telluride nanofluids by 15.27% and 2.07%, respectively. Shen et al. [27] reviewed the applications and effectiveness of these models in enhancing heat transfer across various industries. Khan et al. [28] found the exact solution of the fractal-fractional model of Newtonian fluid flow in a horizontal channel. They used the LTT for the possible exact solution of the model. Wang and Khan [29] also used the FFD of Atangan-Baleanu sense to evaluate the fractional model of bank data. Qureshi and Atangana [30] used the FFD in the biomedical field. They evaluated the biological model of diarrhea transmission dynamics under the use of real data. Some other significant research studies on the application of FFD can be seen in the studies [31–33].

This current work in nanofluids is an exciting look at how this new class of material could revolutionize industrial processing. Nanofluids are being hailed as a transformative heat transfer agent for energy storage and cooling applications in modern engineering practice. While their applications seem very promising, the use cases for this type of technology are still being found. This work is intended to extend these limits by investigating the fractal-fractional order nanofluid model in a vertical channel and solving it using integral transform techniques: Laplace transforms and numerical algorithms. Importantly, it advances the fundamental understanding of these fluid properties but also unveils their great potential to enhance efficiency in a variety of industrial processes. To the best of our knowledge, based on existing review works in the scientific fraternity about the fractal-fractional model, none has so far considered study via the present novelty strategy for nanofluid flow through a channel. Hence, to overcome this deficiency in the literature, partially coupled Newtonian nanofluid flow in a channel was considered by the authors. The classical mathematical model of the proposed problem was developed in terms of PDEs, which have been generalized by an operator for FFD to consider differential expressions. The solution to the generalized

model based on LTT is also provided.

2 Physical Description of the Problem

The geometrical illustration of the phenomenon is given in Figure 1. From the figure it can be seen that at $t = 0$, both the fluid and plates are considered stationary, while at $t = 0^+$, the left plate accelerates with the velocity $U_0 H(t)$, which transmits the motion in the fluid, while temperature and concentration of the ternary nanofluid rise to the timedependent temperature and concentration, respectively.

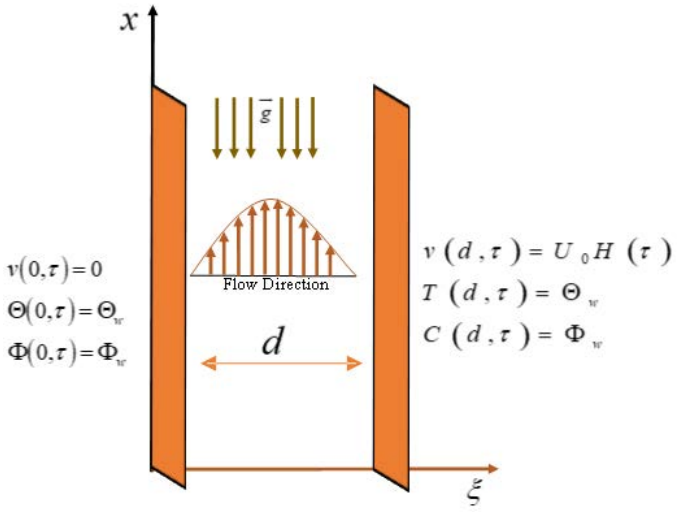

Figure 1. Flow regime

The governing equations for nanofluid flow are given as [24, 25]:

$$\rho_{nf}\frac{\partial v(\xi,\tau)}{\partial t} = \mu_{nf}\frac{\partial^2 v(\xi,\tau)}{\partial y^2} + g\left(\rho\beta_\Theta\right)_{nf}\left(\Theta(\xi,\tau)-\Theta_\infty\right) + g\left(\rho\beta_\Phi\right)_{nf}\left(\Phi(\xi,\tau)-\Phi_\infty\right) \tag{1}$$

$$\left(\rho C_p\right)_{nf}\frac{\partial\Theta(\xi,\tau)}{\partial\tau} = k_{nf}\frac{\partial^2\Theta(\xi,\tau)}{\partial\xi^2} \tag{2}$$

$$\frac{\partial\Phi(\xi,\tau)}{\partial\tau} = D_{nf}\frac{\partial^2\Phi(\xi,\tau)}{\partial\xi^2} \tag{3}$$

IBCs:

$$\left.\begin{array}{llll} v=0, & \Theta=\mathrm{T}_\infty, & \Phi=C_\infty, & \text{at } \xi>0,\tau=0. \\ v=0, & \Theta=\mathrm{T}_\infty, & \Phi=C_\infty, & \text{at } \xi=0,\tau>0. \\ v=UH(\tau), & \Theta=\mathrm{T}_w, & \Phi=C_w, & \text{at } \xi=d,\tau>0. \end{array}\right\} \tag{4}$$

2.1 Dimensional Analysis of the Model

Dimensionless entities are:

$$u=\frac{v}{U},\quad t=\frac{v}{d^2}\tau,\quad y=\frac{\xi}{d},\quad T=\frac{\Theta-\Theta_\infty}{\Theta_w-\Theta_\infty},\quad C=\frac{\Phi-\Phi_\infty}{\Phi_w-\Phi_\infty} \tag{5}$$

Table 1 outlines the mathematical relationships that define the thermophysical properties of the base fluid and the suspended nanoparticles. These relationships are fundamental in bridging the gap between the properties of the regular fluid and those of the nanofluid. By incorporating these expressions, the study effectively transforms the regular fluid model into a comprehensive nanofluid model. This transformation is crucial for accurately investigating the behavior of nanofluid flow, as it accounts for the enhanced thermal and physical characteristics introduced by the suspended nanoparticles. These formulations provide the foundation for analyzing key aspects of nanofluid dynamics, including heat and mass transfer, under various flow conditions.

Table 2 provides a detailed representation of the experimental values of the thermophysical properties for the dispersed nanoparticles, namely Polystyrene, and the base fluid, Kerosene oil. These properties play a crucial role in the subsequent analysis as they serve as fundamental inputs for evaluating the heat and mass transfer rates within the system. By incorporating these experimentally determined values, the study ensures a more accurate and realistic representation of the physical behavior of the nanofluid under investigation.

Table 1. The nanofluid expressions [24]

Properties	Correlations
Density	$\rho_{nf} = (1-\phi_{PS})\,\rho_{KO} + \phi_{PS}\rho_{PS}$
Viscosity	$\mu_{nf} = \frac{\mu_{KO}}{(1-\phi_{PS})^{2.5}}$
Volumetric Expansion	$(\rho\beta_\Theta)_{nf} = (\rho\beta_\Theta)_{KO}\,(1-\phi_{PS}) + \phi_{PS}\,(\rho\beta_\Theta)_{PS}$
Specific Heat Capacity	$(\rho C_p)_{nf} = (1-\phi_{PS})\,(\rho C_p)_{KO} + \phi_{PS}\,(\rho C_p)_{PS}$
Thermal Conductivity	$k_{nf} = k_{KO}\left[\frac{k_{PS}+2k_{KO}-2\phi_{PS}(k_{KO}-k_{PS})}{k_{PS}+2k_{KO}+\phi_{PS}(k_{KO}-k_{PS})}\right]$
Mass Diffusivity	$D_{nf} = D_{KO}\,(1-\phi_{PS})$

Table 2. Experimental values of base fluid and nanoparticles

Properties	$\boldsymbol{\rho}\,(\mathbf{kgm^{-3}})$	$\boldsymbol{C_p}\,(\mathbf{kg^{-1}k^{-1}})$	$\boldsymbol{k}\,(\mathbf{Wm^{-1}k^{-1}})$	$\boldsymbol{\beta}\times 10^{-5}\,(\mathbf{k^{-1}})$
Kerosene Oil	780	2090	0.5	0.9
Polystyrene Nano Particles	1.05	1.4	0.038	0.8

Using the expression given in Table 1 and variables in Eq. (5), Eqs. (1), (2), (3), and (4) will take the form:

$$\frac{\partial u(y,t)}{\partial t} = C_4\frac{\partial^2 u(y,t)}{\partial y^2} + Gr_0 T(y,t) + Gm_0 C(y,t) \tag{6}$$

$$\frac{\partial T(y,t)}{\partial t} = \lambda\frac{\partial^2 T(y,t)}{\partial y^2} \tag{7}$$

$$\frac{\partial C(y,t)}{\partial t} = \lambda_1\frac{\partial^2 C(y,t)}{\partial y^2} \tag{8}$$

and

$$\left.\begin{array}{ll} u = T = C = 0, & \text{at } t = 0, y > 0. \\ u = T = C = 0, & \text{at } t > 0, y = 0. \\ u = H(t), T = C = 1, & \text{at } t > 0, y = 1. \end{array}\right\} \tag{9}$$

During the dimensional analysis, the following physical dimensionless parameters were obtained:

$$Gr = \frac{g\,(\beta_\Theta)_f\,d^2\,(\Theta_w - \Theta_\infty)}{Uv_f}, \quad Gm = \frac{g\,(\beta_\Phi)_f\,\ell^2\,(C_w - C_\infty)}{Uv_f}, \quad Pr = \frac{\mu_f C_p}{k_f}, \quad Sc = \frac{v_f}{D_f}, \quad \delta(t)$$

where, Gr represents the thermal Grashof number, Gm represents the mass Grashof number, Pr represents the Prandtl number, Sc represents the Schmidt number, and $\delta(t)$ is the differential operator.

The following constants emerged during the dimensional analysis process:

$$\lambda = \frac{a_2}{Pr}, a = \frac{1}{\lambda\cdot\beta\Gamma(\beta)}, \lambda_1 = \frac{b_0}{Sc}, b = \frac{1}{\lambda_1\cdot\beta\Gamma(\beta)}, d_0 = \frac{1}{c_4\cdot\beta\Gamma(\beta)},$$
$$\gamma = \alpha+\beta, d_1 = a-d_0, d_2 = b-d_0, Gr_0 = Gr\cdot c_5, Gr_1 = \frac{Gr_0}{c_4}, Gr_2 = \frac{Gr_0}{d_1},$$
$$Gm_0 = Gm\cdot c_6, Gm_1 = \frac{Gm_0}{c_4}, Gm_2 = \frac{Gm_1}{d_1}, c_4 = \frac{c_1}{c_0}, c_5 = \frac{c_2}{c_0}, c_6 = \frac{c_3}{c_0}$$

Since the mathematical model includes nanofluid correlations, it is evident that some of the constants depend on these correlations. The following constants are influenced by the nanofluid correlations:

$$a_0 = (1-\phi_{PS}) + \phi_{PS}\frac{(\rho c_p)_{PS}}{(\rho c_p)_{KO}}, \quad a_1 = \frac{k_{PS}+2k_{KO}-2\phi_{PS}\,(k_{KO}-k_{PS})}{k_{PS}+2k_{KO}+2\phi_{PS}\,(k_{KO}-k_{PS})}, \quad b_0 = (1-\phi_{PS}),$$
$$c_0 = (1-\phi_{PS}) + \phi_{PS}\frac{(\rho)_{PS}}{(\rho)_{KO}}, \quad c_1 = (1-\phi_{PS})^{-2.5}, \quad c_2 = (1-\phi_{PS}) + \phi_{PS}\frac{(\rho\beta_\Theta)_{PS}}{(\rho\beta_\Theta)_{KO}},$$
$$c_3 = (1-\phi_{PS}) + \phi_{PS}\frac{(\rho\beta_\phi)_{PS}}{(\rho\beta_\phi)_{KO}}$$

2.2 Generalization of the Model

The fractal-fractional formulation of the mathematical model is given by:

$$ {}^{FF}D_t^{\alpha,\beta}u(y,t) = C_4\frac{\partial^2 u(y,t)}{\partial y^2} + Gr_0T(y,t) + Gm_0C(y,t) \tag{10}$$

$$ {}^{FF}D_t^{\alpha,\beta}T(y,t) = \lambda\frac{\partial^2 T(y,t)}{\partial y^2} \tag{11}$$

$$ {}^{FF}D_t^{\alpha,\beta}C(y,t) = \lambda_1\frac{\partial^2 C(y,t)}{\partial y^2} \tag{12}$$

where, ${}^{FF}D_t^{\alpha,\beta}$ is the fractal-fractional operator with exponential kernel, which is briefly explained in the study [24].

In a more simplified form, Eqs. (11), (12), and (13) take the form as follows:

$$ {}_{FF}D_t^{\alpha,\beta}u(y,t) + \frac{u(y,0)}{\Gamma(1-\alpha)}t^{-\alpha} = \beta t^{\beta-1}\left\{C_4\frac{\partial^2 u(y,t)}{\partial y^2} + Gr_0T(y,t) + Gm_0C(y,t)\right\} \tag{13}$$

$$ {}^{FF}D_t^{\alpha,\beta}T(y,t) + \frac{T(y,0)}{\Gamma(1-\alpha)}t^{-\alpha} = \beta t^{\beta-1}\left\{\lambda\frac{\partial^2 T(y,t)}{\partial y^2}\right\} \tag{14}$$

$$ {}^{FF}D_t^{\alpha,\beta}C(y,t) + \frac{C(y,0)}{\Gamma(1-\alpha)}t^{-\alpha} = \beta t^{\beta-1}\left\{\lambda_1\frac{\partial^2 C(y,t)}{\partial y^2}\right\} \tag{15}$$

2.3 Solution of the Fractal Fractional Model

Applying integral transform technique on Eqs. (13)-(15), we can get Eqs. (16)-(18):

$$ \hbar^{\alpha}u(y,\hbar) - u(y,0)\left(1 + \frac{\hbar^{-\alpha}\Gamma(1-\alpha)}{\Gamma(1-\alpha)}\right) = \beta\Gamma(\beta)\hbar^{-\beta} * \begin{pmatrix} C_4\frac{\partial^2 u(y,\hbar)}{\partial y^2} \\ +Gr_0T(y,\hbar) + Gm_0C(y,\hbar)\end{pmatrix} \tag{16}$$

$$ \hbar^{\alpha}T(y,\hbar) - T(y,0)\left(1 + \frac{\hbar^{-\alpha}\Gamma(1-\alpha)}{\Gamma(1-\alpha)}\right) = \beta\Gamma(\beta)\hbar^{-\beta} * \left(\lambda\frac{\partial^2 T(y,\hbar)}{\partial y^2}\right) \tag{17}$$

$$ \hbar^{\alpha}C(y,\hbar) - C(y,0)\left(1 + \frac{\hbar^{-\alpha}\Gamma(1-\alpha)}{\Gamma(1-\alpha)}\right) = \beta\Gamma(\beta)\hbar^{-\beta} * \left(\lambda_1\frac{\partial^2 C(y,\hbar)}{\partial y^2}\right) \tag{18}$$

with

$$ \left.\begin{array}{ll} u = T = C = 0, & \text{at } \hbar = 0, y > 0. \\ u = T = C = 0, & \text{at } \hbar > 0, y = 0. \\ u = T = C = \frac{1}{\hbar}, & \text{at } \hbar > 0, y = 1. \end{array}\right\} \tag{19}$$

Incorporating initial conditions given in Eq. (19), we can get Eqs. (20)-(22):

$$ \hbar^{\alpha}u(y,\hbar) = \beta\Gamma(\beta)\hbar^{-\beta} * \begin{pmatrix} C_4\frac{\partial^2 u(y,\hbar)}{\partial y^2} \\ +Gr_0T(y,\hbar) + Gm_0C(y,\hbar)\end{pmatrix} \tag{20}$$

$$ \hbar^{\alpha}T(y,\hbar) = \beta\Gamma(\beta)\hbar^{-\beta} * \left(\lambda\frac{\partial^2 T(y,\hbar)}{\partial y^2}\right) \tag{21}$$

$$ \hbar^{\alpha}C(y,\hbar) = \beta\Gamma(\beta)\hbar^{-\beta} * \left(\lambda_1\frac{\partial^2 C(y,\hbar)}{\partial y^2}\right) \tag{22}$$

By solving Eqs. (20)-(22), we can get Eqs. (23)-(25):

$$u(y,\hbar)=\left[\frac{1}{\hbar}+\frac{Gr_2}{\hbar^{\gamma+1}}+\frac{Gm_2}{\hbar^{\gamma+1}}\right]\frac{\sinh\left(y\sqrt{d_0\hbar^{\gamma}}\right)}{\sinh\left(\sqrt{d_0\hbar^{\gamma}}\right)}-\frac{1}{\hbar^{\alpha+1}}\left[\frac{Gr_2\sinh\left(y\sqrt{a\cdot\hbar^{\gamma}}\right)}{\sinh\left(\sqrt{a\cdot\hbar^{\gamma}}\right)}+\frac{Gm_2\sinh\left(y\sqrt{b\cdot\hbar^{\gamma}}\right)}{\sinh\left(\sqrt{b\cdot\hbar^{\gamma}}\right)}\right] \tag{23}$$

$$T(y,\hbar)=\frac{1}{\hbar}\cdot\frac{\sinh\left(y\sqrt{a\cdot\hbar^{\gamma}}\right)}{\sinh\left(\sqrt{a\cdot\hbar^{\gamma}}\right)} \tag{24}$$

$$C(y,\hbar)=\frac{1}{\hbar}\cdot\frac{\sinh\left(y\sqrt{b\cdot\hbar^{\gamma}}\right)}{\sinh\left(\sqrt{b\cdot\hbar^{\gamma}}\right)} \tag{25}$$

Eqs. (23), (24), and (25) are very complex and difficult to solve by any integral transform means. It is therefore possible to find the inversion form using Zakian's numerical algorithm [34].

$$u(\zeta,t)=\frac{2}{t}\sum_{t=1}^{5}\mathbb{R}e\left\{k_i\bar{u}\left(\zeta,\frac{\alpha_i}{t}\right)\right\} \tag{26}$$

2.4 Nusselt and Sherwood Numbers

The Nusselt and Sherwood numbers are [24]:

$$Nu=-\left.\frac{k_{nf}}{k_f}\frac{\partial T}{\partial y}\right|_{y=0} \tag{27}$$

$$S_h=-D_{nf}\left(\frac{\partial C}{\partial y}\right)_{y=0} \tag{28}$$

3 Graphical and Tabular Analysis

The generalized model of nanofluid has been investigated in a microchannel of length d. The nanofluid mixture has been formed by the uniform dispersion of polystyrene nanocomposite in a base fluid of kerosene oil. The classical model has been generalized by implementing the operator of FFD with a non-singular kernel. The Tiwari and Das nanofluid correlations have been used for developing the nanofluid model. The generalized governing equations have been solved by the integral transform technique, and then for their inversion, a numerical Zakian's algorithm has been applied for the final solution. The impact of rooted parameters has been portrayed in the following.

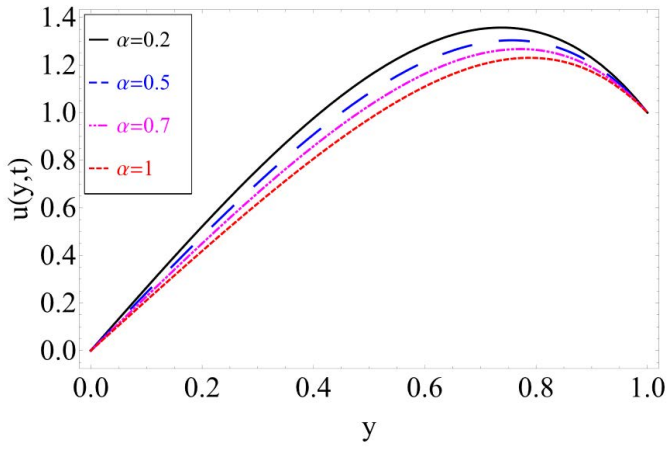

Figure 2. Variation in velocity field against α

The influence of the fractional order on the velocity, thermal, and concentration profiles is presented in Figure 2. From the figure, it is evident that the velocity profile increases with the fractional order. Specifically, the profile

exhibits a growing trend as the fractional order increases. The fractional derivative is employed to capture the memory effect of the fluid. To analyze this memory effect, the fractional derivative is used by substituting the time fractional derivative operator for the classical time derivative in the governing equations.

While the impact of the fractal order on the velocity profile is illustrated in Figure 3, the figure clearly shows that the velocity profile exhibits increasing trends as the fractal dimension increases. This trend indicates that higher values of the fractal dimension led to a more pronounced effect on the velocity distribution across the flow. The fractal dimension plays a crucial role in describing the irregularities and complexities within the fluid flow structure, and it can significantly influence the velocity profile by altering the flow dynamics. As the fractal dimension increases, the flow becomes more sensitive to changes in the geometric and physical properties of the system, thereby modifying the velocity distribution. These changes in the velocity profile suggest that the fractal dimension is an important parameter in understanding and predicting the behavior of fluid flow, particularly in systems where complex geometries or irregular structures are present.

Figure 4 and Figure 5, respectively, show how the thermal Grashof number Gr and mass Grashof number Gm influence the velocity profile. Both figures show increasing variations in the fluid velocity profile for greater magnitudes of Gr and Gm. The Grashof number represents the comparison of the magnitude of buoyancy forces to viscous forces in a fluid flow. Which can influence the velocity profile in a thermal flow. As the values of Gr increase, the buoyancy forces become more significant and make the flow unstable, leading to a greater velocity difference between the top and bottom of the fluid. Therefore, an increasing trend in the velocity profile is observed. The same physical argument is also valid in the case of higher values of Gm.

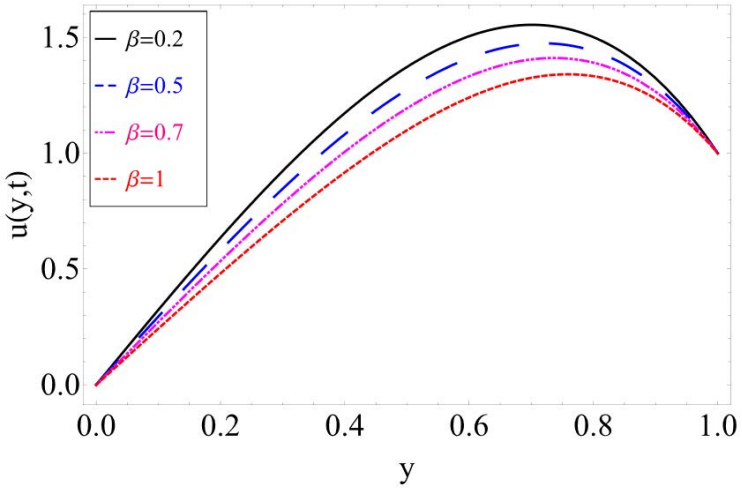

Figure 3. Velocity profile against fractal dimension β

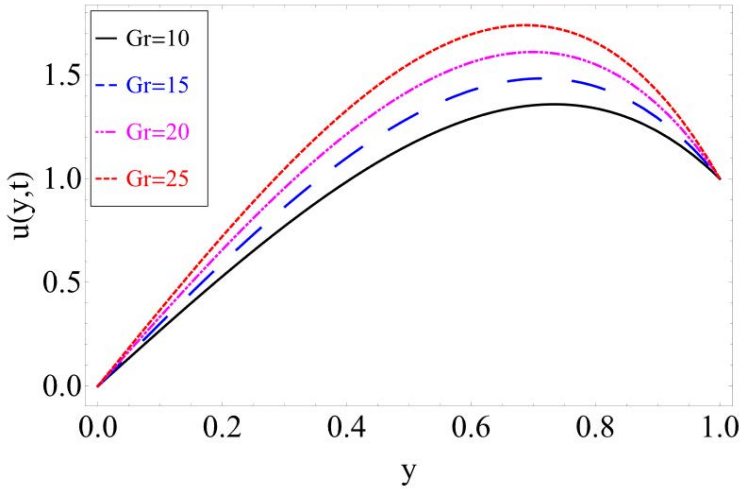

Figure 4. Variation in velocity field against Gr

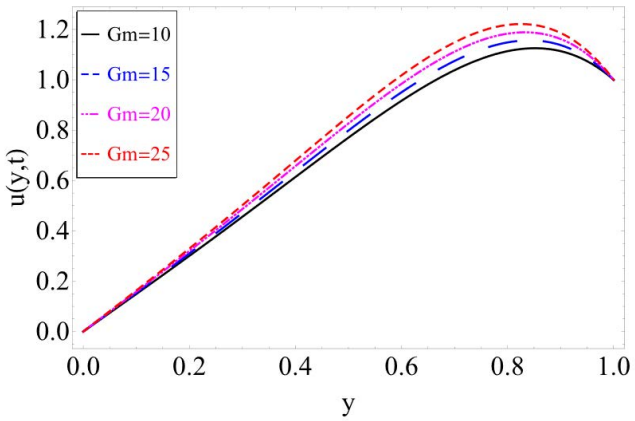

Figure 5. Variation in velocity field against Gm

Figure 6 has been drawn to see the impact of volume fraction ϕ on the velocity profile. Nanoparticles are nanosized solid particles; therefore, the addition of these particles increases the resistance to the fluid flow. This phenomenon is known as the 'Stokes' law.' According to this law, the increased surface area in contact with the fluid caused by the addition of nanoparticles causes a fluid's viscosity to increase. The fluid's flow slows down and the velocity profile drops as viscosity rises. Therefore, a decreasing profile is observed for a higher value of volume fraction. Figures 7 and 8 are presented to examine the influence of the fractional and fractal order on the heat distribution profile. The trend observed is similar to that seen in Figures 2 and 3.

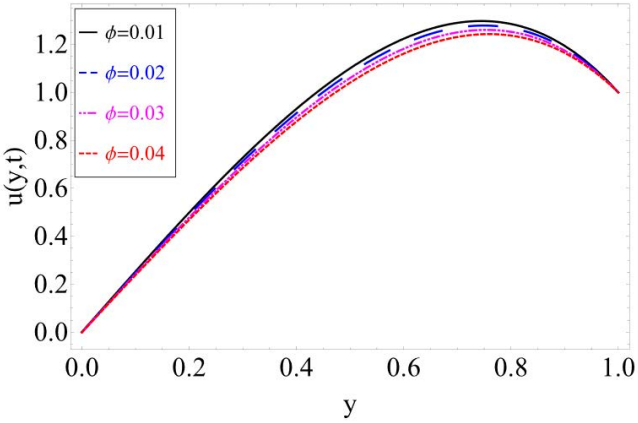

Figure 6. Variation in velocity field against ϕ

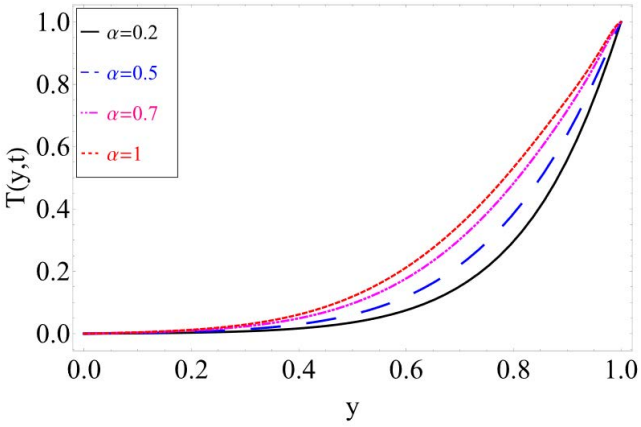

Figure 7. Variation in temperature field against α

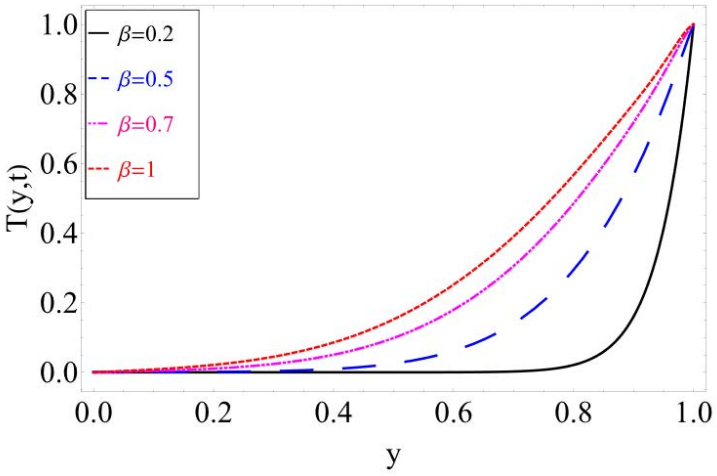

Figure 8. Variation in temperature field against β

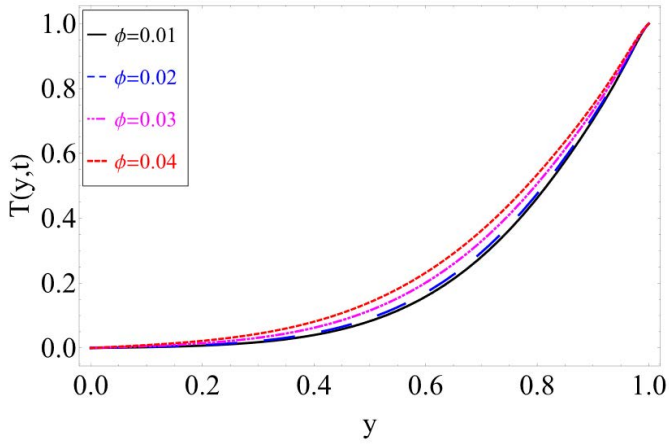

Figure 9. Variation in temperature field against ϕ

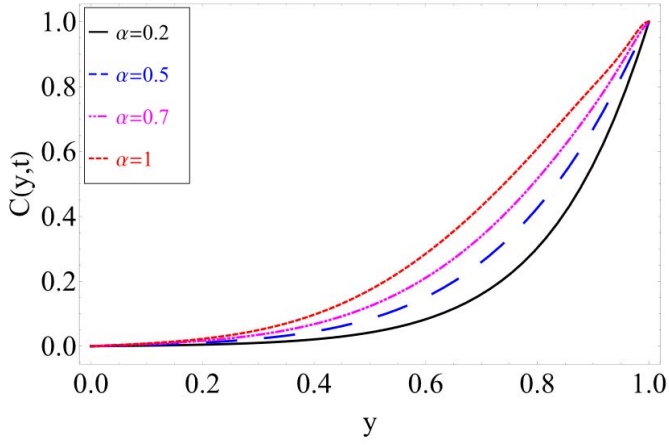

Figure 10. Variation in concentration field against α

Figure 9 shows how the thermal profile varies against the volume fraction of polystyrene nanoparticles. The integral curves in the figure reveal an upward trend when the volume fraction ϕ is increased. This upward trend in thermal profile is because of the advancement in the thermophysical properties of the base fluid. The distributed polystyrene nanoparticles improve specific heat capacity, density, concentration level, viscosity, etc., of regular kerosene oil, thereby enhancing its performance and leading to increased heat distribution. Figures 10 and 11 are presented to examine the influence of the fractional and fractal order on the mass diffusion profile. The trend observed

is similar to that seen in Figures 2 and 3.

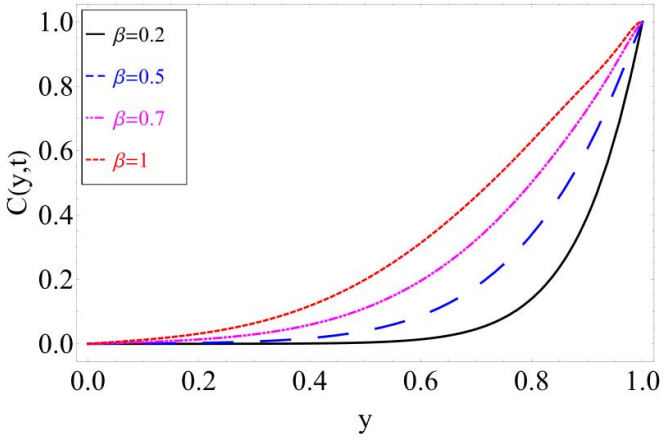

Figure 11. Variation in concentration field against β

Figure 12 illustrates the effect of volume fraction ϕ on the concentration profile. As observed, the concentration profile increases in response to higher values of ϕ. When the volume fraction of polystyrene nanoparticles is increased, the nanoparticles occupy more space within the matrix (such as a polymer, liquid, or solid). This higher particle density results in an increased concentration of nanoparticles within the same volume of the material.

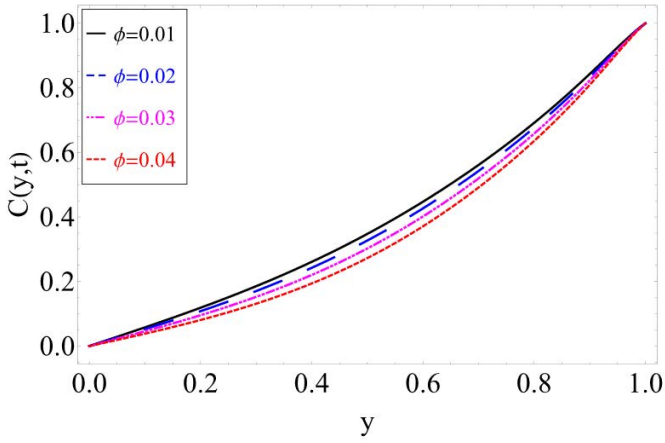

Figure 12. Variation in concentration field against ϕ

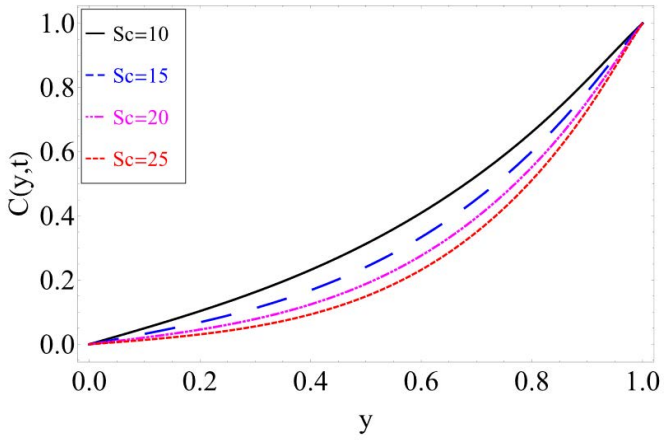

Figure 13. Variation in concentration field against Sc

Figure 13 shows the impact of Schmidt number Sc on concentration profile. High Schmidt number represents

significantly slower diffusion of mass as compared to momentum diffusion. This slower mass diffusion results in a substantial concentration gradient across the boundary, generating a steep concentration profile; therefore, a drop in the fluid's concentration is observed. To examine the impact of volume fraction ϕ (polystyrene nanoparticle) on heat and mass transfer in kerosene oil, Table 3 has been calculated. The tables indicated the variation in both Nusselt and Sherwood numbers but in opposite directions when the volume fraction ϕ reaches 0.04 (4%). The Nusselt number increased by 3.62% while the Sherwood number decreased by 5.68% for 4% of polystyrene nanoparticles. These variations lead to enhanced lubrication properties of the regular kerosene oil.

Table 3. Variations in Nusselt and Sherwood numbers against volume fraction ϕ

ϕ	Nu	Heat Transfer Enhancement	Sh	Decrease in Mass Distribution
0.00	0.573398		0.947399	
0.01	0.567924	0.95465 %	0.934007	1.413554 %
0.02	0.562633	1.87740 %	0.920572	2.831647 %
0.03	0.557225	2.82055 %	0.907094	4.254279 %
0.04	0.552598	3.62749 %	0.893573	5.681449 %

4 Concluding Remarks

We have used the integral transform approach and the numerical Zakian's algorithm to examine a generalized model of nanofluid. The partially coupled mathematical model has been developed in terms of PDEs. For the generalization of the classical mathematical model, the fractal-fractional differential operator of non-singular exponential kernels is employed. The generalized governing equations have been solved by the integral transform technique, and then for their inversion, a numerical Zakian's algorithm has been applied for the final solution. The following are the primary conclusions of the current findings:

• Fractal-fractional operators provide multiple integral curves for the analysis of fluid behavior.

• Analysis shows that the applied numerical scheme is very handy to handle partially coupled PDEs.

• The graphical results indicate that the velocity profile is an increasing function of parameters α, β, Gr and Gm and a decreasing function of parameter ϕ.

• From the analysis, it is concluded that the heat distribution within the fluid increases with the parameter ϕ.

• It is also worthy from the graphical results that the concentration boundary layer shows a decreasing trend in its profile against parameters ϕ and Sc.

• The system's heat transfer rate increases significantly when the volume fraction of polystyrene nanoparticles is increased to 0.04 . Adding 4% polystyrene nanoparticles results in a considerable increase of 3.62% in heat transfer rate.

• When the volume fraction of polystyrene nanoparticles approaches 0.04, the mass transfer rate significantly reduces to 5.68%, suggesting that the mechanism of mass transfer improves at this point.

Data Availability

The data used to support the research findings are available from the corresponding author upon request.

Conflicts of Interest

The authors declare no conflict of interest.

References

[1] E. Kelpsiene, M. T. Ekvall, M. Lundqvist, O. Torstensson, J. Hua, and T. Cedervall, "Review of ecotoxicological studies of widely used polystyrene nanoparticles," *Environ. Sci. Processes Impacts*, vol. 24, no. 1, pp. 8–16, 2022. https://doi.org/10.1039/d1em00375e

[2] O. Mahian, L. Kolsi, M. Amani, P. Estellé, G. Ahmadi, C. Kleinstreuer, J. S. Marshall, M. Siavashi, R. A. Taylor, H. Niazmand, S. Wongwises, T. Hayat, A. Kolanjiyil, A. Kasaeian, and I. Pop, "Recent advances in modeling and simulation of nanofluid flows-Part I: Fundamentals and theory," *Phys. Rep.*, vol. 790, pp. 1–48, 2019. https://doi.org/10.1016/j.physrep.2018.11.004

[3] S. Chakraborty and P. K. Panigrahi, "Stability of nanofluid: A review," *Appl. Therm. Eng.*, vol. 174, p. 115259, 2020. https://doi.org/10.1016/j.applthermaleng.2020.115259

[4] C. Loos, T. Syrovets, A. Musyanovych, V. Mailänder, K. Landfester, G. U. Nienhaus, and T. Simmet, "Functionalized polystyrene nanoparticles as a platform for studying bio–nano interactions," *Beilstein J. Nanotechnol.*, vol. 5, no. 5, pp. 2403–2412, 2014. https://doi.org/10.3762/bjnano.5.250

[5] O. Lunov, T. Syrovets, C. Loos, J. Beil, M. Delacher, K. Tron, G. Ulrich Nienhaus, A. Musyanovych, V. Mailänder, K. Landfester, and T. Simmet, "Differential uptake of functionalized polystyrene nanoparticles by human macrophages and a monocytic cell line," *ACS Nano*, vol. 5, no. 3, pp. 1657–1669, 2011. https://doi.org/10.1021/nn2000756

[6] N. R. Yacobi, L. DeMaio, J. Xie, S. F. Hamm-Alvarez, Z. Borok, K. Kim, and E. D. Crandall, "Polystyrene nanoparticle trafficking across alveolar epithelium," *Nanomed. Nanotechnol. Biol. Med.*, vol. 4, no. 2, pp. 139–145, 2008. https://doi.org/10.1016/j.nano.2008.02.002

[7] C. Oslakovic, T. Cedervall, S. Linse, and B. Dahlbäck, "Polystyrene nanoparticles affecting blood coagulation," *Nanomed. Nanotechnol. Biol. Med.*, vol. 8, no. 6, pp. 981–986, 2012. https://doi.org/10.1016/j.nano.2011.12.001

[8] A. Maestro, E. Guzmán, F. Ortega, and R. G. Rubio, "Contact angle of micro- and nanoparticles at fluid interfaces," *Curr. Opin. Colloid Interface Sci.*, vol. 19, no. 4, pp. 355–367, 2014. https://doi.org/10.1016/j.cocis.2014.04.008

[9] J. Zhang, Y. Song, and D. Li, "Electrokinetic motion of a spherical polystyrene particle at a liquid-fluid interface," *J. Colloid Interface Sci.*, vol. 509, pp. 432–439, 2018. https://doi.org/10.1016/j.jcis.2017.09.020

[10] R. Saboori, S. Sabbaghi, A. Kalantariasl, and D. Mowla, "Improvement in filtration properties of water-based drilling fluid by nanocarboxymethyl cellulose/polystyrene core–shell nanocomposite," *J. Petrol. Explor. Prod. Technol.*, vol. 8, no. 2, pp. 445–454, 2018. https://doi.org/10.1007/s13202-018-0432-9

[11] Q. Li, Y. Lai, P. Li, X. Liu, Z. Yao, J. Liu, and S. Yu, "Evaluating the occurrence of polystyrene nanoparticles in environmental waters by agglomeration with alkylated ferroferric oxide followed by micropore membrane filtration collection and Py-GC/MS analysis," *Environ. Sci. Technol.*, vol. 56, no. 12, pp. 8255–8265, 2022. https://doi.org/10.1021/acs.est.2c02033

[12] F. Mebarek-Oudina, Preeti, A. S. Sabu, H. Vaidya, R. W. Lewis, S. Areekara, A. Mathew, and A. I. Ismail, "Hydromagnetic flow of magnetite–water nanofluid utilizing adapted Buongiorno model," *Int. J. Mod. Phys. B*, vol. 38, no. 1, 2023. https://doi.org/10.1142/s0217979224500036

[13] S. Li, R. Saadeh, J. K. Madhukesh, U. Khan, G. K. Ramesh, A. Zaib, B. C. Prasannakumara, R. Kumar, A. Ishak, and E. M. Sherif, "Aspects of an induced magnetic field utilization for heat and mass transfer ferromagnetic hybrid nanofluid flow driven by pollutant concentration," *Case Stud. Therm. Eng.*, vol. 53, p. 103892, 2024. https://doi.org/10.1016/j.csite.2023.103892

[14] M. Ajmal, R. Mehmood, N. S. Akbar, and T. Muhammad, "Optimizing heat transfer with electro-osmotic ciliated propulsion in a non-uniform canals with Cu-blood characteristics considering thermal casson nano fluid," *Case Stud. Therm. Eng.*, vol. 61, p. 104971, 2024. https://doi.org/10.1016/j.csite.2024.104971

[15] H. A. Nabwey, A. M. A. EL-Hakiem, W. A. Khan, A. M. Rashad, and G. Sayed, "Heat and mass transport micropolar Maxwell and Williamson nanofluids flow past a perpendicular cylinder using combined convective flow," *Chem. Eng. J. Adv.*, vol. 19, p. 100637, 2024. https://doi.org/10.1016/j.ceja.2024.100637

[16] M. T. Usman, M. Abbas Hashmi, S. Nadeem, M. N. J. Baig, M. S. Rashad, J. Alzabut, and H. A. Ghazwani, "Exact solutions of a hybrid nanofluid model for the flow across a heated stretching cylinder at a stagnation point," *J. Nanomater. Nanoeng. Nanosyst.*, 2024. https://doi.org/10.1177/23977914241265549

[17] S. Murtaza and Z. Ahmad, "Analysis of clay based cementitious nanofluid subjected to newtonian heating and slippage conditions with constant proportional Caputo derivative," *GeoStruct Innov.*, vol. 2, no. 2, pp. 53–67, 2024. https://doi.org/10.56578/gsi020201

[18] S. Murtaza, P. Kumam, Z. Ahmad, M. Ramzan, I. Ali, and A. Saeed, "Computational simulation of unsteady squeezing hybrid nanofluid flow through a horizontal channel comprised of metallic nanoparticles," *J. Nanofluids*, vol. 12, no. 5, pp. 1327–1334, 2023. https://doi.org/10.1166/jon.2023.2020

[19] I. Siddique, M. Nadeem, M. M. M. Jaradat, and Z. M. Yaseen, "Impact of fuzzy volume fraction on unsteady stagnation-point flow and heat transfer of a third-grade fuzzy hybrid nanofluid over a permeable shrinking/stretching sheet," *Eng. Appl. Comput. Fluid Mech.*, vol. 18, no. 1, 2024. https://doi.org/10.1080/19942060.2024.2381618

[20] P. Agarwal, R. Jain, and K. Loganathan, "Thermally radiative flow of MHD Powell-Eyring nanofluid over an exponential stretching sheet with swimming microorganisms and viscous dissipation: A numerical computation," *Int. J. Thermofluids*, vol. 23, p. 100773, 2024. https://doi.org/10.1016/j.ijft.2024.100773

[21] P. Bathmanaban, E. P. Siva, S. S. Santra, S. S. Askar, A. Foul, and S. Nandi, "Heat and mass transfer in double-diffusive mixed convection of Casson fluid: Biomedical applications," *Colloid Polym. Sci.*, vol. 302, no. 10, pp. 1635–1669, 2024. https://doi.org/10.1007/s00396-024-05286-3

[22] A. Atangana and E. F. D. Goufo, "Cauchy problems with fractal–fractional operators and applications to groundwater dynamics," *Fractals*, vol. 28, no. 8, 2020. https://doi.org/10.1142/s0218348x20400435

[23] S. Murtaza, P. Kumam, Z. Ahmad, T. Seangwattana, and I. E. Ali, "Numerical analysis of newly developed

fractal-fractional model of Casson fluid with exponential memory," *Fractals*, vol. 30, no. 5, 2022. https://doi.org/10.1142/s0218348x2240151x

[24] S. Murtaza, P. Kumam, T. Sutthibutpong, P. Suttiarporn, T. Srisurat, and Z. Ahmad, "Fractalfractional analysis and numerical simulation for the heat transfer of ZnO+ Al2O3+ TiO2/DW based ternary hybrid nanofluid," *J. Appl. Math. Mech.*, vol. 104, no. 2, 2023. https://doi.org/10.1002/zamm.202300459

[25] Asifa, T. Anwar, P. Kumam, K. Sitthithakerngkiet, and S. Muhammad, "A fractal–fractional model-based investigation of shape influence on thermal performance of tripartite hybrid nanofluid for channel flows," *Numer. Heat Transfer Part A*, vol. 85, no. 2, pp. 155–186, 2023. https://doi.org/10.1080/10407782.2023.2209926

[26] S. Murtaza, P. Kumam, A. Kaewkhao, N. Khan, and Z. Ahmad, "Fractal fractional analysis of non linear electro osmotic flow with cadmium telluride nanoparticles," *Sci. Rep.*, vol. 12, no. 1, 2022. https://doi.org/10.1038/s41598-022-23182-0

[27] M. Shen, H. Chen, M. Zhang, F. Liu, and V. Anh, "A comprehensive review of nanofluids with fractional derivatives: Modeling and application," *Nanotechnol. Rev.*, vol. 11, no. 1, pp. 3235–3249, 2022. https://doi.org/10.1515/ntrev-2022-0496

[28] D. Khan, G. Ali, A. Khan, I. Khan, Y. Chu, and K. S. Nisar, "A new idea of fractal-fractional derivative with power law kernel for free convection heat transfer in a channel flow between two static upright parallel plates," *Comput. Mater. Continua*, vol. 65, no. 2, pp. 1237–1251, 2020. https://doi.org/10.32604/cmc.2020.011492

[29] W. Wang and M. A. Khan, "Analysis and numerical simulation of fractional model of bank data with fractal–fractional Atangana–Baleanu derivative," *J. Comput. Appl. Math.*, vol. 369, p. 112646, 2020. https://doi.org/10.1016/j.cam.2019.112646

[30] S. Qureshi and A. Atangana, "Fractal-fractional differentiation for the modeling and mathematical analysis of nonlinear diarrhea transmission dynamics under the use of real data," *Chaos Soliton. Fract.*, vol. 136, p. 109812, 2020. https://doi.org/10.1016/j.chaos.2020.109812

[31] K. B. Kachhia, "Chaos in fractional order financial model with fractal–fractional derivatives," *Partial Differ. Equ. Appl. Math.*, vol. 7, p. 100502, 2023. https://doi.org/10.1016/j.padiff.2023.100502

[32] Z. Ali, F. Rabiei, K. Shah, and T. Khodadadi, "Modeling and analysis of novel COVID-19 under fractal-fractional derivative with case study of Malaysia," *Fractals*, vol. 29, no. 1, 2021. https://doi.org/10.1142/s0218348x21500201

[33] A. Raza, R. Ali, S. M. Eldin, S. H. Alfalqui, and A. H. Ali, "New fractional approach for CMC and water based hybrid nanofluid with slip boundary layer: Applications of fractal fractional derivative," *Case Stud. Therm. Eng.*, vol. 49, p. 103280, 2023. https://doi.org/10.1016/j.csite.2023.103280

[34] V. Zakian, "Numerical inversion of Laplace transform," *Electron. Lett.*, vol. 5, no. 6, pp. 120–121, 1969. https://doi.org/10.1049/el:19690090